Food Chemistry: X 13 (2022) 100207

Contents lists available at ScienceDirect

Food Chemistry: X

journal homepage: www.sciencedirect.com/journal/food-chemistry-x

Dendrobium officinale leaf polysaccharides ameliorated hyperglycemia and promoted gut bacterial associated SCFAs to alleviate type 2 diabetes in adult mice

Jingyu Fang [a], Yang Lin [a], Hualing Xie [a], Mohamed A. Farag [b,c], Simin Feng [a], Jinjun Li [d], Ping Shao [a,e,*]

[a] Department of Food Science and Technology, Zhejiang University of Technology, Zhejiang, Hangzhou 310014, China
[b] Pharmacognosy Department, College of Pharmacy, Cairo University, Kasr El Aini St., Cairo, 11562, Egypt
[c] Department of Chemistry, School of Science & Engineering, The American University in Cairo, New Cairo 11835, Egypt
[d] Institute of Food Science, Zhejiang Academy of Agricultural Sciences, Hangzhou 310021, China
[e] Key Laboratory of Food Macromolecular Resources Processing Technology Research, China National Light Industry, Hangzhou 310021, China

ARTICLE INFO

Keywords:
Dendrobium officinale
Intestinal microflora
Polysaccharide
Short-chain fatty acids
Type 2 Diabetes

ABSTRACT

The present study aimed to explore the possible mechanisms underlying *Dendrobium officinale* leaf polysaccharides of different molecular weight to alleviate glycolipid metabolic abnormalities, organ dysfunction and gut microbiota dysbiosis of T2D mice. An ultrafiltration membrane was employed to separate two fractions from *Dendrobium officinale* leaf polysaccharide named LDOP-A and LDOP-B. Here, we present data supporting that oral administration of LDOP-A and LDOP-B ameliorated hyperglycemia, inhibited insulin resistance, reduced lipid concentration, improved β-cell function. LDOP-A with lower molecular weight exhibited improved effect on diabetes than LDOP-B, concurrent with increased levels of colonic short-chain fatty acids (SCFAs) i.e., butyrate, decreased ratio of Firmicutes to Bacteroidetes phyla, and increased abundance of the gut beneficial bacteria i.e., *Lactobacillus*, *Bifidobacterium* and *Akkermansia*. These results suggest that LDOP-A possesses a stronger effect in ameliorating T2D than LDOP-B which may be related to the distinct improved SCFAs levels produced by the change of intestinal flora microstructure.

Introduction

Type 2 Diabetes (T2D), characterized by lack of insulin or inability of peripheral tissues to respond to insulin adequately, is growing in incidence and prevalence worldwide (Moini, 2019). Besides hyperglycemia, the T2D phenotype often exhibits hyperlipidemia, dysfunction of energy metabolism and heart disease, and kidney failure (Fan & Pedersen, 2021). With further research on the relationship between intestinal microbiota and host metabolic health, the change in structure of gut microbiota has been suggested to be closely related with the occurrence and development of T2D (Fan & Pedersen, 2021). Some researchers have demonstrated that T2D is associated with a depletion in bacterial butyrate producers, and with relative increase in the ratio of Firmicutes to Bacteroidetes phyla (Gastaldelli, Gaggini, & DeFronzo, 2017; Lee et al., 2019). In fact, some of the anti-hyperglycemic effects of metformin, the most commonly used anti-diabetes drugs is mediated *via* the enhanced production of short chain fatty acids (SCFAs) and unconjugated bile acids in the intestine and subsequent activation of intestinal gluconeogenesis (Sun et al., 2018). Several studies also suggest that short-chain fatty acid receptors FFA2 (GPR43) and FFA3 (GPR41) have been implicated in metabolic diseases such as type 2 diabetes and in regulation of appetite. (Kobayashi et al., 2017)

In recent years, increasing interest has been given towards the use of natural bioactives in plant materials to prevent and treat T2D owing to

Abbreviations: AUC, The area under the concentration–time curve; FBG, fasting blood glucose; FT-IR, Fourier-transform infrared; GLP-1, glucagon-like peptide-1; GLUT4, glucose transporter type 4; H&E, hematoxylin and eosin; HDL-c, high-density lipoprotein cholesterol; HFD, high-fat diet; HOMA-IR, homeostasis model assessment-insulin resistance; HOMA-β, β-cell sensitivity; IC, ion Chromatography; IL-6, interleukin-6; LDL-c, low-density lipoprotein cholesterol; LDOP, *Dendrobium officinale* leaf polysaccharide; Mw, molecular weight; OGTT, oral glucose tolerance test; OTUs, operational taxonomic units; PAS, periodic acid-Schiff; PYY, peptide YY; SCFAs, short chain fatty acids; STZ, streptozotocin; T2D, Type 2 Diabetic; TG, triglycerides; TNF-α, tumor necrosis factor-alpha.

* Corresponding author.
E-mail address: pingshao325@zjut.edu.cn (P. Shao).

https://doi.org/10.1016/j.fochx.2022.100207
Received 12 June 2021; Received in revised form 17 November 2021; Accepted 5 January 2022
Available online 10 January 2022

their relative safety. Some natural plant polysaccharides are indigestible carbohydrates with complex molecular structures, mostly digested and utilized by colonic microorganisms (Xie et al., 2018). Several studies have investigated the natural polysaccharides in diet found to decrease fasting blood glucose, insulin, glycated serum protein, serum lipids level (Chen et al., 2019; Gao et al., 2018). Moreover, polysaccharide interventions have been suggested as a beneficial method in altered gut microbiota linked with the promotion of the beneficial bacteria proliferation, increased concentrations of SCFAs, regulation of cytokines expression and improvements of energy metabolism (Kjolbaek et al., 2020). Consequently, changes in intestinal microflora regulated by polysaccharides have also become a new target in the prevention and treatment of T2D. The connection between T2D amelioration and changes in colon flora change induced by polysaccharides remains to be completely deciphered.

Dendrobium officinale (stems), an important edible-medicinal plant enriched in polysaccharides as the main bioactive ingredient found to act as prebiotic properties and alleviate symptoms related to diabetes (Kuang et al., 2020). Typically, *Dendrobium officinale* leaves are considered a waste with considerable biomass and recently found to encompass chemical constituents similar to those found in stems suggestive for its medicinal value (Liu et al., 2020). Whether polysaccharide extracted from *Dendrobium officinale* leaves exhibit a similar effect to that in stems for T2D treatment has yet to be determined (Hsieh et al., 2008). Furthermore, accumulating evidence have shown that the molecular weight (Mw) of the polysaccharides affect their hypoglycemic ability and fermentation ability. For example, insulin and its low molecular derivatives have different butyrate-producing ability (Pylkas et al., 2005). Similarly, differential SCFA levels was observed from the fermentation of guar gum with different molecular weights (Fu et al., 2019). However, there is no report on the difference in structure and molecular weight of *Dendrobium officinale* leaf polysaccharide involved in microbiological digestion metabolism and its impact on subsequent functions.

Our previous study revealed that oral administration of 200 mg/kg/day *Dendrobium officinale* leaf aqueous extract altered intestinal flora with significant positive immunoregulatory effects. In the present study, the hypoglycemic effect and modulation of fat and glucose homeostasis of two LDOPs with different molecular weight were systematically confirmed herein, as evidenced by decreased FBG level, increased glucose tolerance and the improvement of pancreas, liver and colon function in a high-fat diet (HFD) and streptozotocin (STZ)-induced diabetic mice. The effect of LDOPs on microbiota composition and production of SCFAs were also investigated, and its relationships with diabetes management were inter related.

Materials and methods

Materials

Dendrobium officinale leaves were collected from Yueqing county (Wenzhou, China) in July of 2020. Metformin (BR, 97%) was obtained from Sangon Biotech Co., Ltd (Shanghai, China). DEAE Cellulose-52 was purchased from Yuanye Bio-Technology Co., Ltd (Shanghai, China) and Sephadex G-200 was purchased from Aladdin Bio-Chem Technology Co., Ltd (Shanghai, China). Dextran standards (5000, 11600, 23800, 48600, 80900, 148000, 273000, 409800, 667800 Da), STZ (≥75% α-anomer basis), glucose (AR, 99%), and insulin (BR, 27U/mg) were all purchased from Sigma-Aldrich (Missouri, USA). Antibodies against GRP43, insulin and glucagon as well as their isotype control antibodies were purchased from Proteintech (Chicago, USA). GRP41 and GAPDH antibodies was purchased from Abcam (Cambridge, USA). Acetic acid, propionic acid, butyric acid, isobutyric acid, valeric acid, and isovaleric acid (≥99.5) were purchased from Thermo Fisher Scientific (Waltham, USA).

LDOPs preparation and composition detection

Polysaccharide was extracted as previously described with a slight modification (Ke et al., 2020). After grinding, the leaves of *Dendrobium officinale* were soaked in 85% ethanol for 12 h in the ratio of 1:20 (w/v), for 3 times. Then filter by suction, and the filter residue was dried in the fume hood. The dried powder was extracted twice by magnetic stir with distilled water (1:30, w/v) at 70℃, each for 2 h. After centrifugation at 5000g for 20 min, the protein in supernatant was removed with Sevag's method. Retained aqueous phase was concentrated, and a five-fold volume of anhydrous ethanol was slowly added to the concentrated solution and stored overnight at 4℃. The floccule precipitate obtained after centrifugation at 5000g for 10 min was lyophilized to obtain the crude polysaccharide (LDOP).

LDOP was resuspended in distilled water and separated by ultrafiltration (Xie et al., 2014). Continuous ultrafiltration was carried out through the membrane with the membrane cartridge of 100 kDa (PES10-1812), under the pressure of 0.5 MPa and flow rate of 30 L/h until maximum permeate yield was reached. Permeate and retentate solution (LDOP-A permeate, LDOP-B retentate) were collected separately and lyophilized same as above. Three milligrams of two polysaccharide solution (20 mg/mL) were loaded on an anion DEAE Cellulose-52 column (1.6 × 60 cm), followed by elution with distilled water and 0.4 mol/L NaCl solution sequentially at a flow rate of 1 mL/min. The same fractions from each sample were combined, concentrated, and then dialyzed (1000 Da MWCO). Two polysaccharides fraction was further purified through a Sephadex G-200 column (0.5 mL/min flow rate with distilled water and 0.3 mol/L NaCl solution), yielding the polysaccharides LDOP-A and LDOP-B after lyophilization.

Total sugar content was determined by measuring eluent absorbance at 490 nm according to the phenol–sulfuric acid method, using glucose as a standard (Rao & Pattabiraman, 1989). Total flavonoid content was measured using the method detailed by Kim, Jeong, and Lee (Tomas et al., 2018). The polyphenol content was determined via the Folin–Ciocalteu assay (Fecka et al., 2021). The absorbances of the solutions above were determined spectrophotometrically with GENESYS 150 ultraviolet–visible spectrophotometer (Thermo Scientific, USA).

HPLC, FTIR and SEM analysis

The molecular weight of LDOP-A and LDOP-B were determined according to the method of Chen et al (2018). High-performance liquid chromatography (LC-10A, Shimadzu, Japan) equipped with a refractive index detector (RI-10A, Shimadzu, Japan) was used to determine the retention times of samples. The BRT105-104–102 (8 × 300 mm) column was eluted with NaCl solution (0.05 M) flow rate of 0.6 mL min^{-1}. The linear regression curve was calibrated using the dextran standards. The calibration curve of glycans (lgMw-RT: $y = -0.1985x + 12.509$, $R^2 = 0.9964$) is calculated. The molecular weight of LDOP-A and LDOP-B was calculated from the above calibration curve.

The monosaccharide composition was determined using HPLC as previously described with some modifications (Yang et al., 2020b). Dried samples (100 mg) were dissolved in 5 mL of 2 M trifluoroacetic acid (TFA). The mixed solution was hydrolyzed at 120 °C for 2 h. After the solution was cooled to room temperature, the reaction mixture was purged by N_2 to remove TFA and the residue was redissolved in 4 mL of ultrapure water. 1 mL sample solution was mixed with 400 μL of 1-phenyl-3-methyl-5-pyrazalone (PMP) methanol solution (0.5 M) and 400 μL of NaOH solution (0.3 M), left to react in a water bath set at 70 °C for 2 h. Subsequently, the sample solution was washed three times with chloroform following the addition of 500 μL HCl solution (0.3 M), and the supernatant was collected by centrifugation at 500 × g for 20 min. The derivative supernatant was filtered using 0.22 μm membrane and analyzed using HPLC (U3000, ThermoFisher, USA) with C18 column (5 μm, 4.6 mm × 250 mm, Thermo Fisher, USA) and detected using an ultraviolet detector at 245 nm. The HPLC analysis conditions were as

follows: column temperature, 30 °C; mobile phase, 0.1 M phosphate buffer (A, pH = 6.4) and acetonitrile (B); flow rate, 1.0 mL min − 1. The gradient elution program was set as follows: 0–34.5 min, 82% A; 34.5–45 min, 20–50% A; 45–51 min, 50% A; 51–53 min, 50–82% A; 53–58 min, 82% A.

Dried polysaccharide samples (2 mg) were ground with 100–200 mg KBr powder and then pressed into flake for FTIR determination on Nicol et iS50 spectrometer (Thermo Scientific, USA) record FTIR spectrum ranging 4000–500 cm^{-1}.

The morphologies of polysaccharides samples were observed by SEM. Su8020 SEM scanning electron microscope (Hitachi, Japan) was used to observe the sample's surface at 10 kV acceleration voltage and image magnifications of 2000 × .

Animal experiments

LDOP-A/B treatment

Male C57BL/6 mice (7 weeks old, 20 ± 2 g) were obtained from Shanghai SLAC Laboratory Animal Co. Ltd (Shanghai, China). All mice were permitted to drink regularly freely. This experiment was approved by the ethics committee of Zhejiang University of Technology, China.

T2D was induced in mice by a high-fat diet (HFD, 60% energy from fat) together with STZ injection. After a week of adaption, 8-week-old C57BL/6 male mice were fed with normal chow (NC) diet or an HF diet for 56 days. T2D mice were induced as described previously with slight modification (Ru et al., 2020), HF-fed mice were injected with 100 mg/kg body weight of the STZ solution (500 mg/L in 0.1 M citrate–phosphate buffer, pH 4.5) after fasting for 12 h. After 5 and 7 days, the fasting blood glucose (FBG) levels were determined. The mice with FBG levels of two days both > 11.1 mol/L were considered as the T2D mice and randomly divided into four groups (n = 8). After that, each group were all fed with NC diet.

Dosage information

For the treatment, mice were orally administered daily LDOP-A (200 mg/kg/day), LDOP-B (200 mg/kg/day), metformin (200 mg/kg/day) or with saline for the controls for 4 weeks according to a previous study (Ru et al., 2020), which was equivalent to 16.3 mg/kg/d in humans. Polysaccharides and metformin were suspended in distilled water, and then administered by intragastric gavage in a volume of 10 mL/kg.

Sample collection and biomarkers determination

Feces were collected before euthanized and stored at −80 °C for further studies. All mice were fasted for 12 h and anesthetized with 4% chloral hydrate after the last blood glucose test, and blood was taken from the abdominal vein. Blood samples were collected and centrifugation under the condition of 4 ℃, 4000 R/min, for 10 min, the upper serum was taken after centrifugation. The liver, kidney, intestine, fat and muscle tissues were taken, the floating blood on the surface of the tissue was washed with pre-cooled normal saline, the surface of the tissue was dried with filter paper, and the weight was recorded. Colonic contents were also collected in centrifuge tubes and stored at − 80℃ until DNA extraction.

Parameters such as FBG, body weight, food and water intakes were measured weekly. Blood glucose levels were measured by glucometers and test-strips (Accu-Chek, Roche Diagnostics, Switzerland), and the blood was taken from the tail tip with rid of the first drop of blood. Serum total cholesterol (TC), Triglyceride (TG), low-density lipoprotein cholesterol (LDL-c), high-density lipoprotein cholesterol (HDL-c) was assessed by kit (Nanjing Jiancheng Bioengineering Institute, Nanjing, China). Serum insulin concentration was assessed according to the manufacturer's protocol (Nanjing Jiancheng Bioengineering Institute, Nanjing, China).

Glucose tolerance test was performed by oral glucose tolerance test (OGTT) according to (Wang, 2021). A few days before the mice were killed, 5 mice near the average value of blood glucose in each group were selected and orally administrated with glucose at concentration of 1 g/kg BW after fasted for 14 h. The blood glucose level was determined at −60, 0, 15, 30, 60, 90 and 120 min after glucose administration. The glycemic index was calculated by adding the glycemic values from all time points multiplied by the duration of the test. The area under the concentration–time curve (AUC) were calculated for glucose concentration using the trapezoidal method. The homeostasis model assessment-insulin resistance (HOMA-IR) and β-cell sensitivity (HOMA-β) were calculated.

Histolopathological examination

The liver and colon samples were homogenized with PBS buffer (pH = 7.4) and centrifuged at 4℃, 14,000 rpm for 15 min. The supernatant was collected and used to measure inflammatory markers using ELISA assays. Interleukin-6 (IL-6) and tumour necrosis factor α (TNF-α) were determined by ELISA kit (Neobioscience Biotechnology Co., Ltd, Shanghai, China).

According to the reported method (Shang et al., 2021), pancreas, liver and colon of mice were dehydrated, transparentized and embedded in paraffin and cut into slices of 4 μm thick. Subsequently, the pancreas, liver and intestine samples were stained with hematoxylin and eosin (H&E), periodic acid-Schiff (PAS) and oil red O (ORO), respectively. For immunofluorescence staining, the pancreas slices were pre-treated as described above and stained with primary antibodies against insulin and glucagon overnight at 4 ℃. All images were captured under the bright field microscope (Olympus, CX22LED, USA) and analyzed by Image-J software. The severity of T2D was assessed based on a method mentioned in previous published (Moini, 2019).

Determination of SCFAs in feces

GC (Agilent 7890A, USA) is used to determine the SCFAs concentration efficiency. 0.1 g fresh colon content samples were suspended in a phosphoric acid solution (pH = 7.6, 0.01 M, 1 mL). After fully homogeneous and centrifugation at 10,000 rpm/min for 10 min, supernatant was collected and passed through a 0.2 μm aqueous membrane for further analysis. Oven temperature was increased from 60 to 100 ℃ at 5 ℃/min, then to 145 ℃ at 10 ℃/min. The peak area was quantified to mmol/mL and then calculated as mmol/mg feces.

Determination of GPR41 and GPR41 expression

The total protein of colon tissue was extracted by total protein extraction kit (Thermo Scientific Pierce, Shanghai), with the total protein quantified using BCA protein assay kit (Beyotime Biotechnology, Shanghai). Equal amounts of loaded proteins were separated by 10% SDS–PAGE, were then transferred to a PVDF membrane after electrophoresis. Blots were blocked with 5% nonfat dry milk for 1 h at room temperature, and then incubated with a primary antibody (1:1000) for one night at 4℃, followed by incubation with a secondary antibody (1:5000) for 1 h at room temperature. Protein signals were visualized by enhanced chemiluminescence using ECL DualVue WB Marker (General ElectricCo., Shanghai) for 1 min and exposed to X-ray film. Signal intensities of all bands were quantified by densitometry with Image J software.

DNA extraction and 16sRNA sequencing

Microbial genomic DNA of each colon content sample was extracted by a fast DNA stool mini kit (QIAamp, QIAGEN, Germany). After DNA samples were prepared, genomic DNA was extracted by 1% agarose gel electrophoresis and quantified using a Qubit and NanoDrop. The V4 hypervariable regions of the bacteria 16S rRNA gene were amplified by PCR using primers 341F (5′-CCTAYGGGRBGCASCAG-3′) and 806R (5′-GGACTACNNGGGTATCTAAT-3′) (Møller et al., 2013). After purified

with a DNA Purification Kit (TIANGEN, Beijing), Final PCR products were quantified by qubit3.0 fluorometer (Agilent Technologies, USA). The library of mixed samples was constructed by paired-end sequencing (2 × 250 bp) on an Illumina Truseq DNA (San Diego, USA) according to standard protocols (Zhu et al., 2021).

Statistical analysis

Data were analyzed by using Origin 2021 software. The statistical differences between groups were analyzed by one-way analysis of variance (ANOVA) followed by Tukey's multiple-comparisons tests. Significant difference was set as *P < 0.05, **P < 0.01, and ***P < 0.001 for comparison with the model group.

Operational taxonomic units (OTUs) were defined as the minimum of 97% sequence similarity. The alpha diversity was calculated, the OTU table was rarefied at an even sampling depth of 7050 sequences/sample. Species richness was estimated using Chao1and the number of observed species diversity was analyzed using Shannon (Quast et al., 2013). PCA statistical analysis and mapping were performed with R language.

Results

Structural characterization of LDOP-A and LDOP-B

Although the alcohol-soluble substances, proteins and oligosaccharides were removed by pretreatment, the residual constituents with

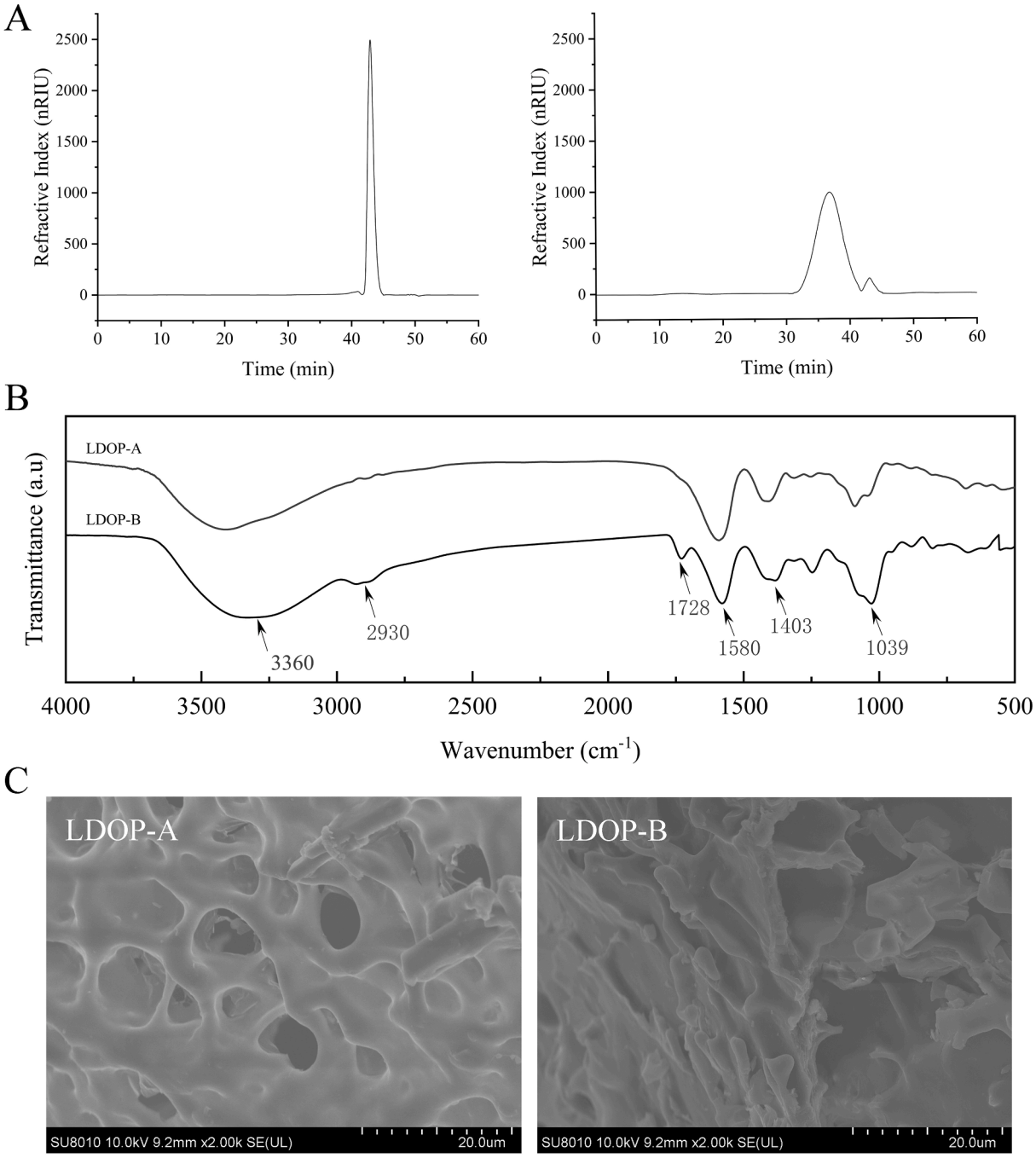

Fig. 1. HPLC, FT-IR spectra and SEM images of LDOP. (A) Mw of LDOP-A and LDOP-B. (B) FT-IR spectra LDOP-A and LDOP-B. (C) SEM images of LDOP-A and LDOP-B.

hypoglycemic function may still remain in LDOPs. Consequently, the composition of LDOP-A and LDOP-B were determined to identify structures or groups mediating for the biological effects. The purity of polysaccharides was determined at 86.34% and 92.21%, respectively, with trace amounts of flavonoids and polyphenols detected in both samples (<0.01%). HPLC result showed LDOP-A being composed of glucose, mannose, glucuronic acid, and galactose at a molar ratio of 3.2:2.6:1.0:0.7. In contrast, LDOP-B was comprised of mannose, glucose, galactose, glucuronic acid, and arabinose at a molar ratio of 8.8:1.0:0.7:0.1:0.1.

As shown in Fig. 1A, only a single peak with a molecular weight of 9.91 kDa was observed in LDOP-A, while in LDOP-B a main peak was detected followed by several smaller peaks, whose average molecular weight was estimated to be 147.45 kDa. The strong absorption characteristic peaks of polysaccharides were detected at 3360 cm^{-1}, 2930 cm^{-1} and 1403 cm^{-1} suggestive for the presence of O—H bond C—H and COO– in both LDOP-A and LDOP-B (Fig. 1B). Weaker 1403 cm^{-1} peak intensity in LDOP-A indicates that there are few β-glucans, which is

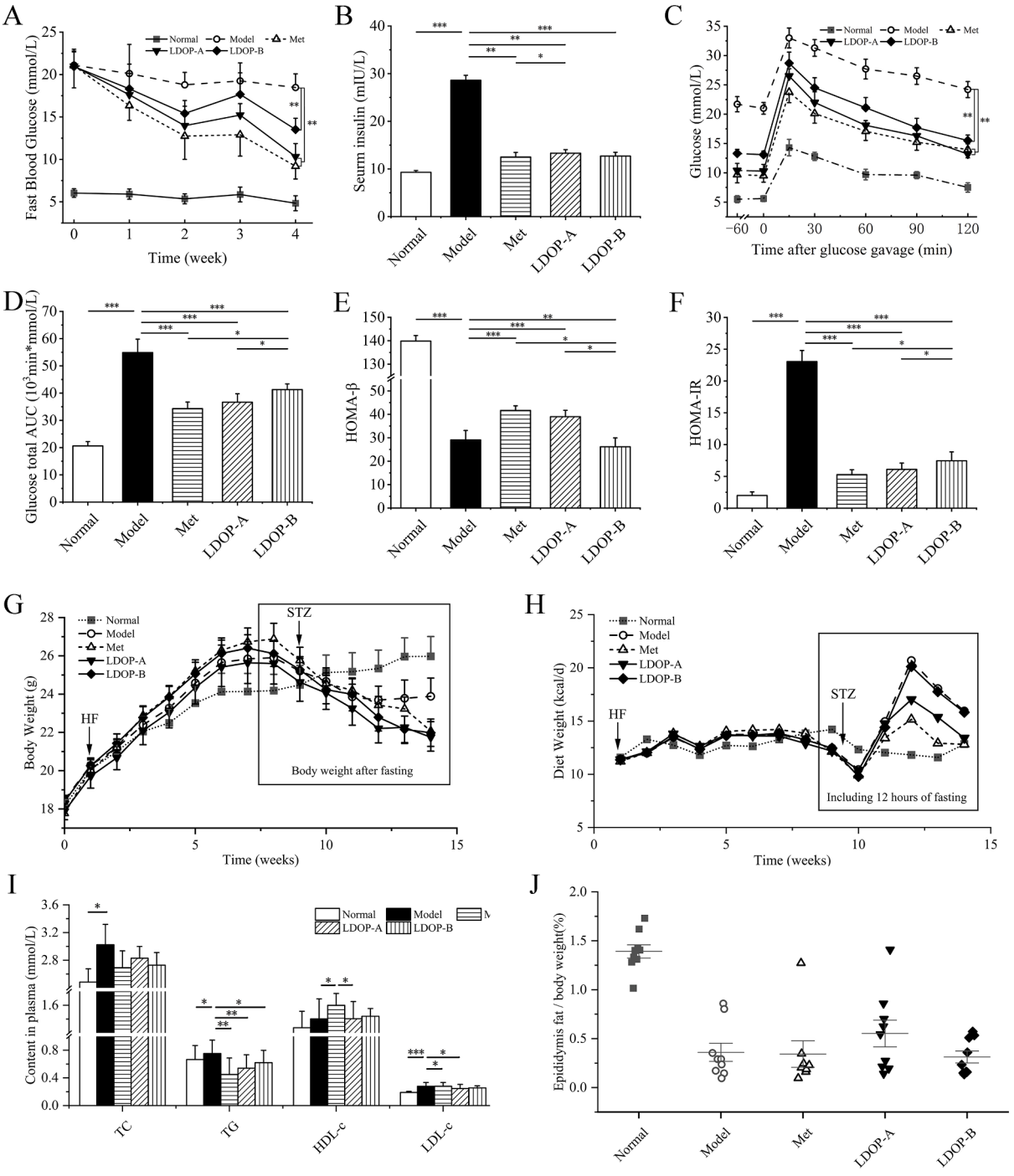

Fig. 2. LDOP improve glucose homeostasis and attenuates changes in serum diabetic biomarkers in T2D mice. (A) Glucose was tested after 6 h fasting (n = 8). (B) Seurm insulin (n = 8). (C) tolerance tests with OGTT (n = 5). (D) total glucose AUC (n = 5). (E) Insulin resistance: HOMA-IR (n = 8). (F) Beta cell sensitivity: HOMA-β (n = 8). (G) Body weight and (H) food intake (n = 8). (I) TC, TG, HDL-c and LDL-c (n = 8). (J) Epididymal fat index (n = 8).

abundant in LDOP-B (Fig. 1B). The tight configuration and micropores of LDOP-A reflect that it may have numerous highly branched polysaccharide chains, while LDOP-B has an irregular shape structure with flat and smooth surface and a few flaky structures (Fig. 1C). Further, detailed characterization of the polymers using other spectroscopic techniques i.e., NMR should aid to provide unequivocal structural assignment of these polymers.

LDOPs ameliorated hyperglycemia and insulin sensitivity in T2D mice and mitigates energy metabolic dysfunction

In order to elucidate the role of LDOP-A and LDOP-B in controlling glucose homeostasis and insulin sensitivity, the FBG levels, insulin level and oral glucose tolerance were measured. Met was used as a positive drug control. Relative to T2D model group, the FBG of 4-week LDOP-A and LDOP-B treated mice were significantly reduced in varying degrees (Fig. 2A, both $p < 0.001$). LDOP-A even achieved a comparable hypoglycemic effect with metformin at the fourth week ($p > 0.05$). Similarly, serum insulin level was also significantly decreased after oral administration of LDOP-A and LDOP-B (by 33.5% and 24.8%, both $p < 0.001$) compared with the model group (Fig. 2B). The oral glucose tolerance of LDOP-A and LDOP-B treated groups were better at individual time points, with AUC during 120 min showing a decrease by 54.2%, 24.8% (Fig. 2C, D), indicating that they can enhance the body's ability to regulate increase in blood glucose level. Compared with model group, LDOP-A-administrated and LDOP-B-administrated mice possess higher

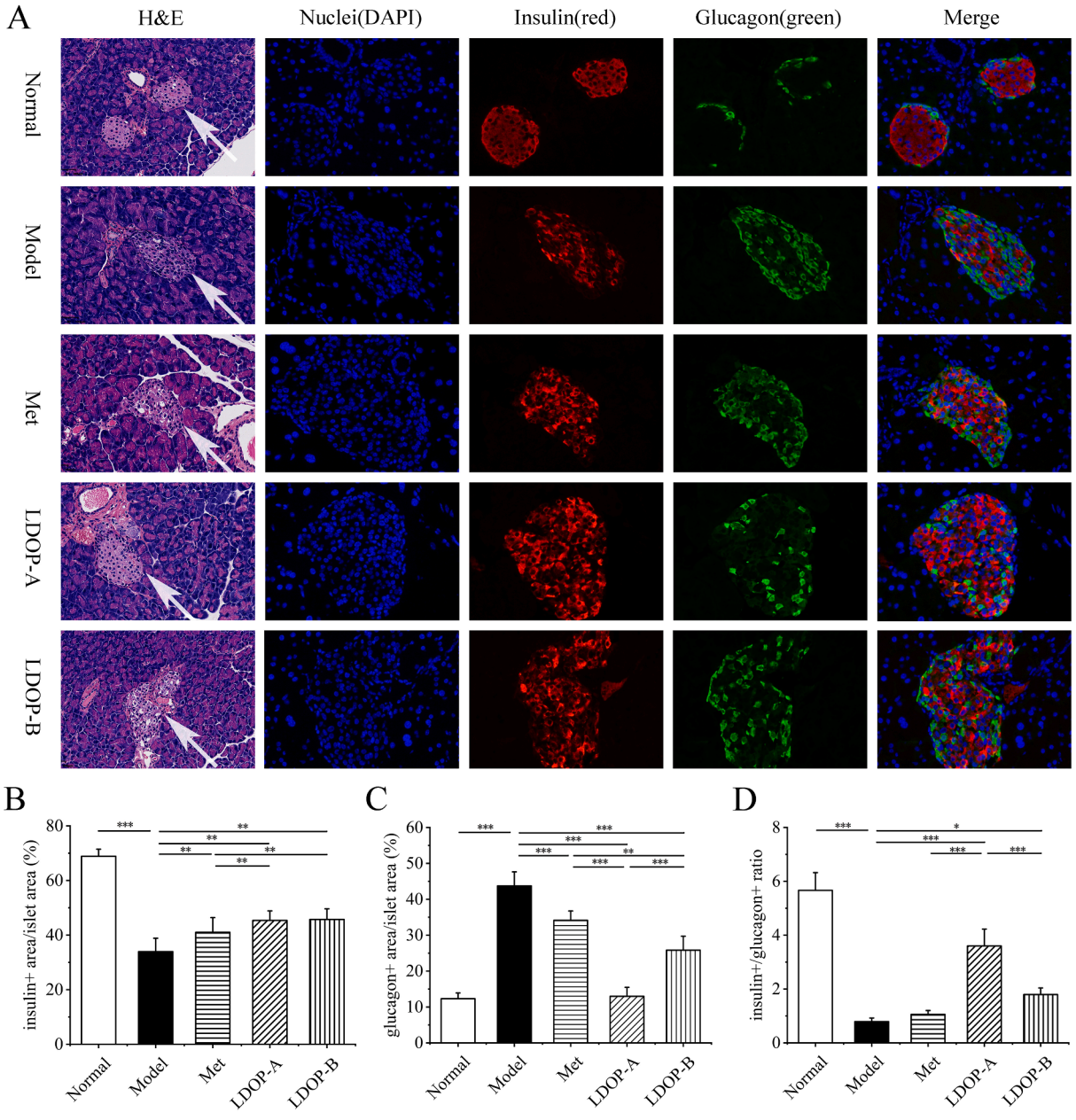

Fig. 3. Restoration of pancreatic islet function by 4-week LDOP administration in T2D mice. (A) Pancreatic tissue was stained with (H&E) and double-immunostained with anti-insulin antibody (red) and anti-glucagon antibody (green) while the nuclei were counterstained with DAPI in blue. (B) The ratio of insulin positive β-cell area to islet area (n = 5). (C) The ratio of glucagon positive α-cells to islet area (n = 5). (D) The ratio of insulin positive β-cell area to glucagon positive α-cells (n = 5). Quantification of islet area was calculated based on H&E staining of pancreatic section. (For interpretation of the references to colour in this figure legend, the reader is referred to the web version of this article.)

HOMA-β (Fig. 2E) and lower HOMA-IR (Fig. 2F).

Since T2D is a systemic metabolic disease, the regulatory effects of LDOP-A and LDOP-B on obesity and dyslipidemia of T2D mice were investigated. After diabetic model was established, many of the metabolic indicators were attenuated or reversed by 4-weeks metformin or the LDOPs administration with marked prevention in rapid body weight and epididymal fat loss (Fig. 2G and J). Meanwhile, metformin showed the most obvious inhibitory effect on appetite of T2D mice, followed by LDOP-A, which shows a significant difference with LDOP-B (Fig. 2H, $p < 0.001$). Both LDOP-A and LDOP-B treatment showed a hyoplipdemic action manifested by decrease in serum lipids (Fig. 2I). Compared with the model group, LDOP-A treatment decreased serum concentration of TG and HDL-c (by 42.2% $p < 0.01$, by 27.4p < 0.05, respectively) and increased the LDL-c levels (by 34.5% $p < 0.05$), while treatment of LDOP-B only reduced that of TG (by 33.3% $p < 0.05$) (Fig. 2I).

LDOPs improved islet morphology and β-cell function in T2D mice

Combined treatment of HFD and STZ is known to cause destruction of β-cells and decrease in the mass of islets (Wang et al., 2019). In the normal mice, islet cells were regularly distributed and uniform in size. In contrast, the size of islet cell was inconsistent, the pancreatic duct was dilated and proliferated in the model group (Fig. 3A). The morphology of pancreas in LDOP-A group was markedly improved, the size of islet cells returned to uniform, and LDOP-B also has a slight role in alleviating the pathological changes (Fig. 3A). Moreover, the quantification of insulin$^+$ β-cell area calculated based on these digitized images showed a 1.07-, 1.34-, and 1.37-fold rise in Met, LDOP-A and LDOP-B compared with model group mice, respectively (Fig. 3B). Contrary to insulin$^+$ β-cell area, LDOP-A and LDOP-B decreased the ratio of glucagon$^+$ α-cells to islet area by 70.3% ($p < 0.001$) and 43.1% ($p < 0.001$) (Fig. 3C). The ratio of insulin$^+$ β-cells area to glucagon$^+$ α-cells area was significantly increased by LDOP-A (4.49 times of the model group, $p < 0.001$), higher than that increased by LDOP-B (2.30 times, $p < 0.05$) and metformin (1.36 times, $p > 0.05$) (Fig. 3D).

LDOPs recovery liver morphology and regulated hepatic glucose metabolism in T2D mice

Next, the effects of LDOPs on the morphology of hepatocytes, glycogen and fat in liver and inflammatory cytokines levels were analyzed to assess its impact on metabolic function of liver (Song et al., 2017). H&E staining showed the liver cells arranged irregularly, round in cell morphology, and extensive vacuolization appeared in the cytoplasm, suggesting that T2D mice induced serious liver injury (Fig. 4A). Staining of the livers with PAS and oil red O (Fig. 4A) revealed a decrease of liver glycogen in hepatocytes of T2D mice and an accumulation of microvesicular fat. These abnormalities mentioned all markedly improved in LDOP-A treated mice and slightly improved in LDOP-B treated mice. Hepatic glycogen content of liver showed a 1.81-, 1.8-, and

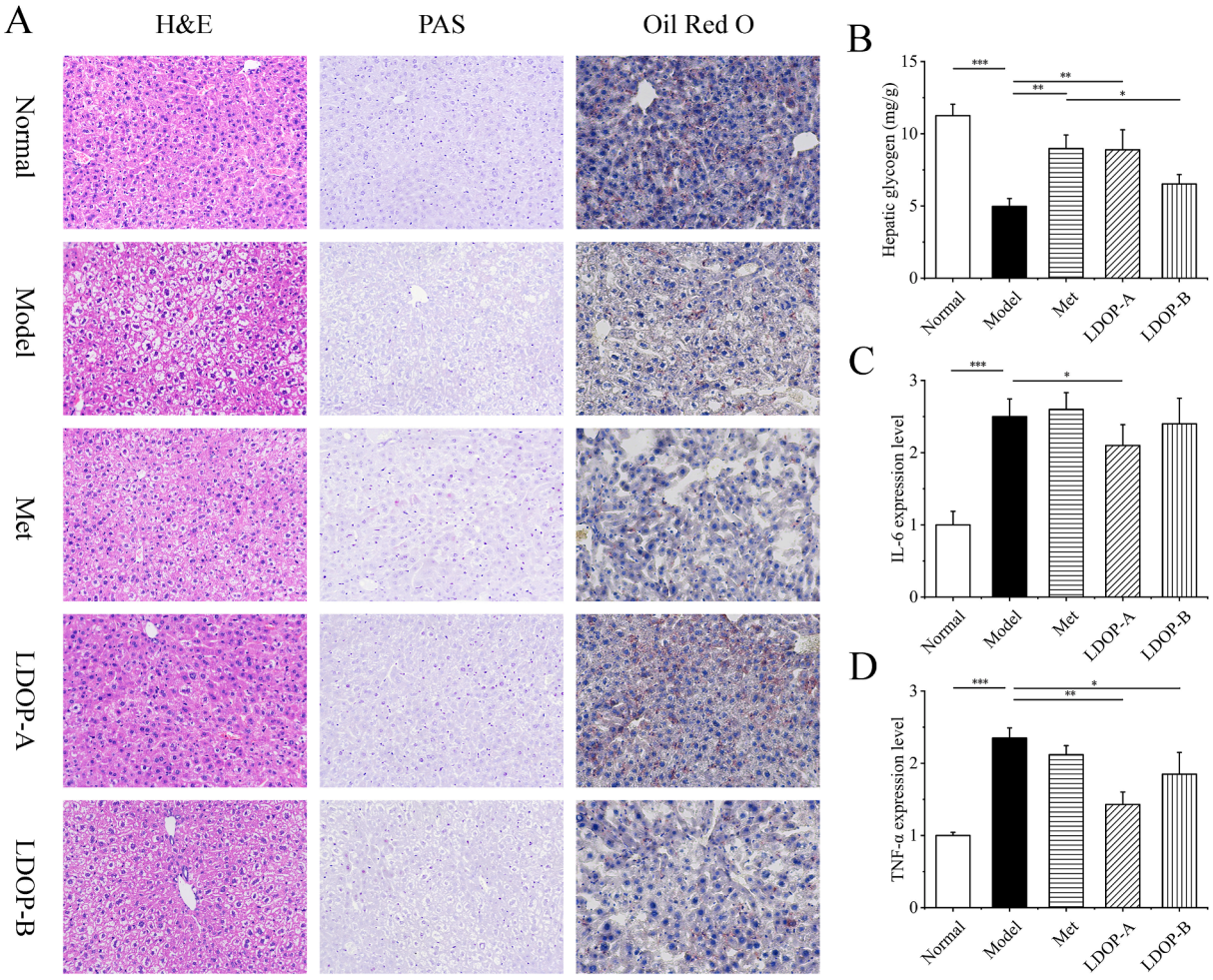

Fig. 4. Effects of LDOP on liver morphology, liver glycogen and liver fat. (A) H&E, PAS, Oil Red O staining of liver. (B) Glycogen content in liver cells (n = 8). (C) Expression level of IL-6 in liver (n = 8). (D) Expression level ofTNF-α in liver (n = 8). (For interpretation of the references to colour in this figure legend, the reader is referred to the web version of this article.)

1.3-fold rise in Met, LDOP-A, and LDOP-B group mice compared with model group mice, respectively (Fig. 5B). Meanwhile, the expression levels of pro-inflammatory cytokines, such as interleukin-6 (IL-6) and tumor necrosis factor-alpha (TNF-α) were increased in model mice. Both IL-6 and TNF-α in LDOP-A group were significantly lowered ($p < 0.05$ and $p < 0.01$), and only TNF-α were lowered in LDOP-B group ($p < 0.05$).

LDOPs upregulates butyrate production accompanied by an increase in the SCFA receptor and enhance intestinal physical barrier in T2D mice

As we know, SCFAs can reduce the pH of the colon, inhibit pathogens, and regulates intestinal mucosal barrier function (Xie et al., 2019). Concentrations of SCFAs in faeces (formic acid, acetic acid, propionic acid, butyric acid, isobutyric acid, valeric acid, and isovaleric acid), as major microbial fermentation products of diets, were measured to display the possible regulation effects of LDOP-A and LDOP-B (Liang et al., 2020). GC analyses revealed that 4 weeks of metformin or LDOP-A treatment restored SCFAs production (by 50.2% and by 48.6%, both $p < 0.05$), which had been reduced in response to diabetes. LDOP-A-treated diabetic mice exhibited more colonic SCFAs content than that in LDOP-B-treated mice (24.03 and 18.11 mmol/mg, respectively) (Fig. 5 A). At the same time, compared with the diabetic group, the fecal butyric acid content of LDOP-A group was significantly increased by 24.5% ($p < 0.05$) (Fig. 5 A). However, there was no significant difference in the amount of total SCFAs and butyric acid content between LDOP-B-treated group and the T2D model group (Fig. 5 A). Receptors for SCFAs, GPR41 and GPR43, were both expressed in L cells in colon and anti-inflammatory effects can be exerted by binding and activating GPR41 and GPR43 (J. Liu et al., 2020). Compared with T2D group, the expression of GPR41 and GPR43 were significantly upregulated in LDOP-A group, while the increase was less evident in case of LDOP-B-treated group (Fig. 5 D, E).

Generally, several common chronic disorders that appear to be characterized by a relative disruption of the gut barrier (Luck et al., 2019). H&E staining showed a small amount of inflammatory cell infiltration in the model diabetic group, but it was not detected in other groups (Fig. 5B). This suggests that both LDOP-A and LDOP-B exhibit anti-inflammatory effects on colon. Furthermore, TNF-α levels of LDOP-A and LDOP-B treated groups were significantly decreased ($p < 0.001$) in the colon, indicating that they might possess the potential to attenuate colon inflammation (Fig. 5C).

LDOPs restores diabetes-induced gut microbial dysbiosis

It was logical to assess how LDOPs alter the global structure of the gut microbiota to evaluate its effect on improving intestinal flora disturbance in T2D. At the phylum level, a significant increase in *Bacteroidetes* abundance (both $p < 0.001$) and a decrease in *Firmicutes* abundance (both $p < 0.001$) was found in LDOP-A and LDOP-B group compared to T2D mice (Fig. 6A, C). However, compared with *Firmicum* to *Bacteroides* ratio 0.84 of LDOP-A, the proportion of LDOP-B was 1.20,

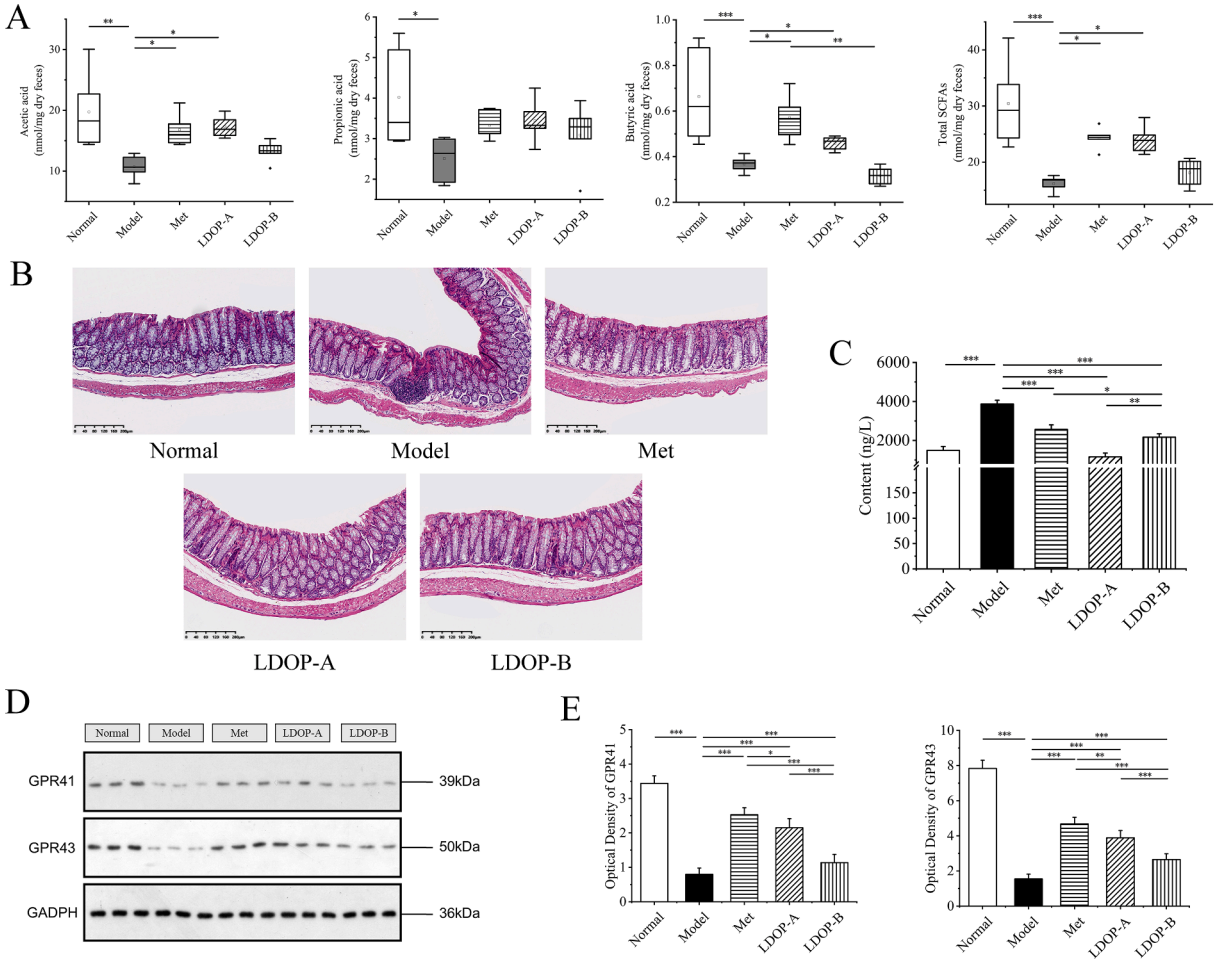

Fig. 5. LDOP upregulates acetic acid, propionic acid and butyric acid production accompanied by an inflammation relief and of colon in T2D diabetic mice. (A) SCFA concentration in faeces measured by GC. Effects of LDOP administration on intestinal mucosal morphology(n = 8). (B) H&E staining of colon. (C) TNF-α in colon and serum(n = 8). (D) Western blot of GPR41 and GPR41. (E) Quantitative analysis of GPR41 and GPR43 expression in western blot.

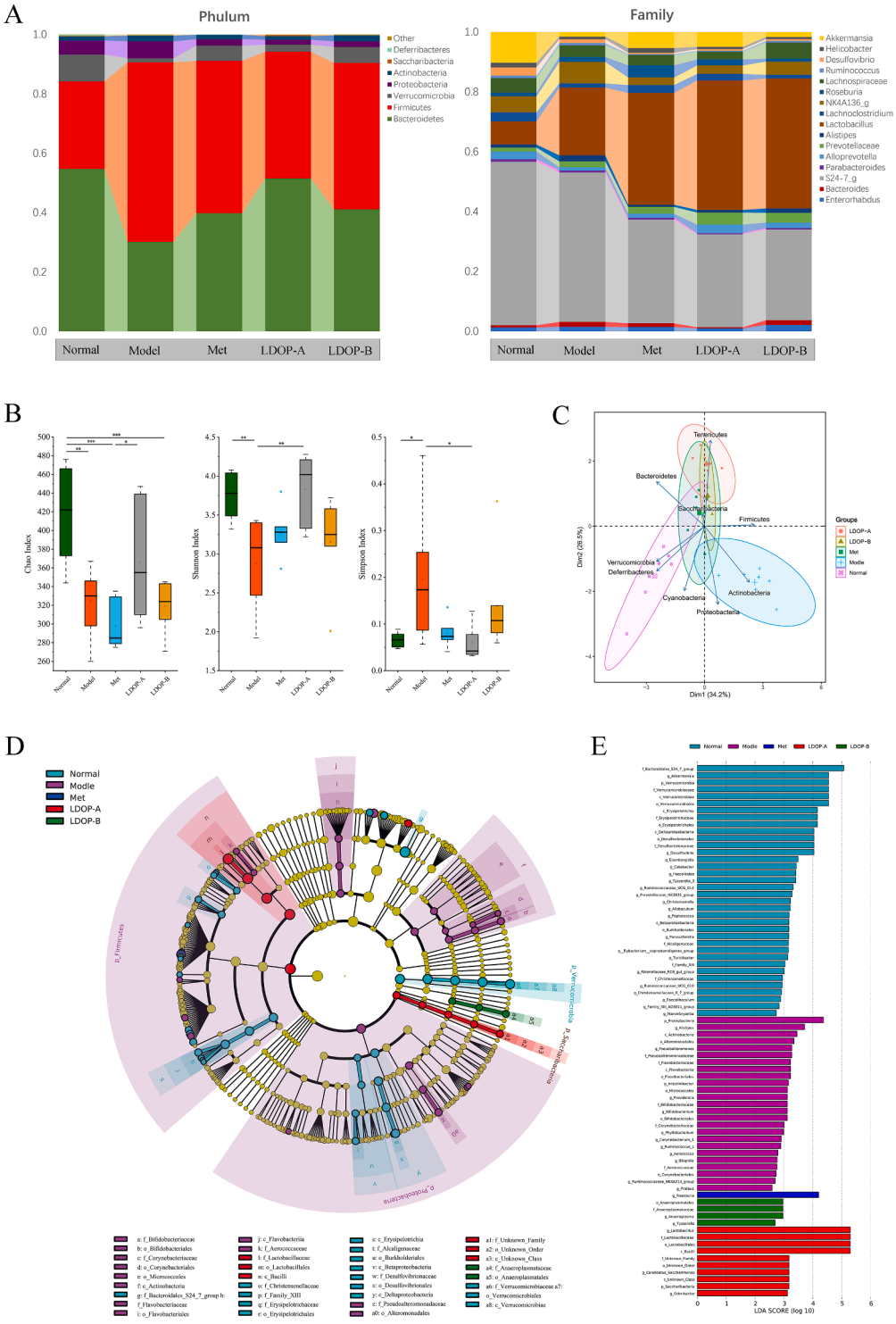

Fig. 6. LDOP restored the diabetes-induced gut microbial dysbiosis at different taxonomic levels in T2D mice. (A) Abundance of the most important phyla and genus in each group(n = 7). (B) Abundance of the main altered classes in each group(n = 7). (C) Principal coordinate analysis (PCA) plot of weighted UniFrac distances, each dot representing a colonic community; the percentage of variation explained by each principal coordinate is shown in parentheses; 95% confidence ellipses covered all samples in their own regions (n = 7). (D) Taxonomic representation of statistically and biologically consistent differences between adequate and excessive groups(n = 7). (E) Histogram of the linear discriminant analysis (LDA) scores for differentially abundant genera(n = 7).

which was less different from 2.01 of the model group. The genus-level analysis revealed that the abundance of *Streptococcus* showed significant increase ($p < 0.001$) while those of *Clostridiales*, *Akkermansia*, *Bifidobacterium* and *Lactobacillus* were decreased by the T2D, and recovered after LDOP-A treatment (Fig. 6A, D).

T2D induce the growth of species with a pro-inflammatory action, such as *Proteobacteria*, *Corynebacteriales* and *Alistipes*, with a significant reduction in the SCFAs-producing taxonomies endotoxin produced by these harmful bacteria can cause inflammation and reduce the sensitivity of the insulin receptor (Shin, Whon, & Bae, 2015). The intervention of metformin significantly increased the abundance of *Roseburia* (Fig. 6D), leading to an increase in the production of butyric acid (Kasahara et al., 2018). Butyric acid has anti-inflammatory effect, which may inhibit the activity of histone deacetylase, leading to histone hyperacetylation, thereby inhibiting activation of nuclear factor- κ B. *Lactobacillus* and *Bifidobacterium* (Fig. 6D), related to revoking insulitis and β-cell destruction associated with increased IL-10 secretion (de Oliveira, 2019), were promoted by LDOP-A. In addition, the OTU of

microbiota in the diabetic group was significantly decreased and to be reversed by the oral administration of LDOP-A but not by LDOP-B (Fig. 6B).

Discussion

We observed changes of gut microbiota composition and derived microbial compounds by interventions of polysaccharide from *Dendrobium officinale* leaves in T2D mice, and its action mechanism in relation to insulin resistance and hypoglycemia in diabetic rats. *Dendrobium officinale* leaves polysaccharides have been extensively investiagated in literature (Ke et al., 2020; Wang, 2021), but to our knowledge, this is the first detailed study to assess the effects of two components of LDOPs with different molecular weights on hyperglycemia and its associated dysfunction, as well as their effect on the gut microbiota in T2D mice.

LDOPs are the most abundant and promising bioactives in *Dendrobium officinale* leaves. Their different polysaccharide structural composition may lead to varies anti-diabetic activities and SCFAs producing effects, exemplified in either monosaccharide type and or glycosidic linkage composition, molecular weight (Pan, 2014). Polysaccharide with different molecular weight (Mw 28.34 kDa, 41.14 kDa and 91.8 kDa) were separated from *Dendrobium officinale* leaves by Zhang et al (Zhang et al., 2018) and Yang et al (Yang et al., 2020b), but their hypoglycemic activities and antidiabetic effect have not been elucidated. Two kinds of *Dendrobium officinale* leaves polysaccharides fractions with different molecular weights (Mw 147.45 kDa and 9.91 kDa, termed LDOP-A and LDOP-B) were obtained by ultrafiltration in this study, and their effects in treatment of T2D in mice have been studied comprehensively (Fig. 1A). Typically, high molecular weight polysaccharides are not conducive to readily cross cell-membranes, and it is more difficult to be consumed with less chance to exert their biological activities (Zhang et al., 2019), and in accordance to our results. Meanwhile, the LDOP-B also exerted strong anti-inflammatory effect inside the colon, which may be due to its high mannose content.

In our study, LDOP-A and LDOP-B were confirmed to improve glucose homeostasis and insulin resistance (Fig. 2C-F), with LDOP-A found more effective than that of LDOP-B. Changes in body weight, food intake and lipogenesis of mice between groups suggested that LDOP-A modulates energy homeostasis of T2D, with effect of LDOP-A better than that of LDOP-B (Fig. 2 G-J). Serum lipids analysis indicated that the disturbing degree of fat (TG, LDL-C, HDL-C) metabolism was mitigated by bothLDOP-A and LDOP-B treatment (Fig. 2I), and in accordance with the results obtained by Yang et al. (2020a). Meanwhile, no dramatic change of body weight and blood sugar be seen with LDOP-A and LDOP-B administration suggesting that LDOP-A and LDOP-B had no obvious toxic effect on mice.

According to the observation of pancreatic staining, LDOP-A and LDOP-B both reduced pancreatic cells damage and protected insulin-producing pancreatic β-cells, even better than that of metformin. LDOP-B has similar proportion of insulin positive area as LDOP-A, but its glucagon^{+} area showed no significant difference with the diabetic group (Fig. 3B, C). The increased liver glycogen level indicates that the LDOP-A treatment lowered hepatic glucose output. LDOP-A also improved liver inflammation and lipid accumulation, which was not observed in LDOP-B group (Fig. 4A). All to conclusively suggestes that LDOP-A may inhibit glycogen decomposition or promote a large amount of blood glucose to synthesize glycogen to reduce blood glucose. Together, these results suggest that LDOP-A may improve host glucose homeostasis involved in biochemical pathways related to glucagon-like peptide 1 (GLP-1)/insulin, glycolysis/gluconeogenesis, lipogenesis and lipid export from the liver (Xie et al., 2020), and protection of impaired islet function and β-cell function is protected from further damage.

Microbial metabolites are important mediators of microbial-host crosstalk impacting host glucose metabolism. At the intestinal level, butyrate plays a regulatory role on the transepithelial fluid transport, ameliorates mucosal inflammation and oxidative status and reinforces the epithelial defense barrier (Canani et al., 2011). T2D patients are characterized by a dramatic decrease in butyrate levels, which has been demonstrated as an important factor in maintaining intestinal health and participating in immune regulation and intestinal barrier function adjustment (Jia et al., 2017). Thus, targeted restoration of the SCFAs production may provide a novel method to manage T2D. The production of acetic acid and butyric acid increase the secretion of GLP-1 and peptide YY (PYY) in the intestine, thus promoting insulin secretion and improving type 2 diabetes (Fan & Pedersen, 2021; Kasahara et al., 2018). Although polysaccharides were difficult to be digested in the gastrointestinal tract, they can be fermented by microorganisms in the colon to regulate the structure of the host's intestinal flora (Ulven, 2012), and likely to moreover exert systemic actions (Elshahed et al., 2021). LDOP-A supplementation modulated colon environment manifested by increase in intestinal immunity and SCFAs level, especially that of butyrate (Fig. 5A). However, the effect of LDOP-B on short chain fatty acids was not significant. It was also reported that FFA2 (GPR43) and FFA3 (GPR41) are activated by acetate, propionate, and butyrate and mediate SCFA-promoted GLP1 release from mixed colonic cultures under *in vitro* conditions (Tolhurst et al., 2011). Supplementation with LDOP-A tripled the expression of GPR41, whereas GPR43 expression was 1.5 times higher than T2D group (Fig. 5 D, E). These observations indicate that LDOP-A have potential as a GPR41 and GPR43 agonist for the treatment of type 2 diabetes and related metabolic diseases. Thus, we speculate that different contents of SCFAs produced by intervention of LDOP-A and LDOP-B may lead to varying degrees of decreasing susceptibility to inflammation inside the colon and improvement of T2D partly *via* bile acid metabolism.

Changes in intestinal bacteria composition can likewise regulate the production of lipopolysaccharide and SCFAs, further affecting the absorption of sugars and energy (Puddu et al., 2014). Based on the obviously different effects of LDOP-A and LDOP-B on hyperglycemic, glucose homeostasis, tissue dysfunction and SCFA production, the impact of LDOP-A and LDOP-B on intestinal flora homeostasis was further assessed as part of this study. Loss of the fragile equilibrium was observed in the diabetic group, termed dysbiosis as manifested by decrease in healthy bacteria concurrent with an increase in the number of harmful bacteria i.e., *Proteobacteria* (Fig. 6 C-E). These may serve as an initiating or reinforcing factor in T2D and whether be used routinely for diabetes prognosis in humans should be considered in the future. LDOP-A exerted an increased effect on the diversity of intestine flora, though with no significant difference between LDOP-B and the diabetic group, which may result in a different effect on other symptoms of T2D mice and likely to also account for results of SCFAs in both LDOP-A and -B treated groups. Except for metformin treatment group, LDOP-A changed the gut microbiota most. LDOP-A group was found lower Firmicutes to Bacteroidetes ratio and higher abundance of beneficial bacteria such as *Akkermansia*, *Bifidobacterium* and *Lactobacillus* than LDOP-B group (Fig. 6 A-E).

Jia et al (2017) reported that a butyrate-producing bacteria supplementation can reverse the tendency of gut butyrate to decrease in mice as induced by HF and streptozotocin, thereby leading to an anti-diabetic effect. Here, we observed that LDOP-A changed the structure of the gut microbiota as evidenced by increased abundance of some beneficial bacteria i.e., *Lactobacillus*, *Bifidobacterium*, *Akkermansia* and some butyrate-producing flora i.e., *Clostridiales*. At the same time, LDOP-B was not found to increase butyrate-producing bacteria and ultimately lead to an increase in butyric acid level (Fig. 6 A, D). To sum up, this suggests that the differential effects between LDOP-A and LDOP-B may be partly attributed to the distinct SCFAs content produced by the change of intestinal flora structure.

Conclusion

In conclusion, two polysaccharides, LDOP-A and LDOP-B, were

separated from LDOP by ultrafiltration, novel effects linking LDOP-A and LDOP-B with alleviated hyperglycemia and other symptoms of T2D were reported. Due to the significant restoration of diabetic syndrome, modification of morphology and function of the islet, liver and colon, reduced levels of inflammation, as well as modulation of gut microbiota composition, LDOP-A and LDOP-B are suggested as a dietary supplement and/or potential drug to alleviate T2D. LDOP-A showed better effects than LDOP-B in controlling fasting blood glucose and hypolipidemic, improving islets and liver function and reducing of inflammation, and finally promoting SCFAs level, especially butyrate, produced by the structural changes of intestinal flora. These results extendthe anti-hyperglycemic effect of *Dendrobium officinale* polysaccharide action mechanisms, classically ascribed to be used for the recovery of islet cells and present an added value for *Dendrobium officinale* leaves polysaccharide in T2D management.

Funding sources

This work was supported by Key Research and Development Projects in Zhejiang (No. 2019C02070, 2021C02019), National Natural Science Foundation of China (No.32072149) and Zhejiang Sci-tech University Shaoxing Biomedical Research Institute Co.LTD.

Compliance with ethics requirements

All Institutional and National Guidelines for the care and use of animals (fisheries) were followed.

All animals used in this study were cared for in accordance with the Guidelines for the Care and Use of Laboratory Animals published by the United States National Institute of Health (NIH, Publication No. 85–23, 1996). This experiment was approved by the ethics committee of Zhejiang University of Technology (Animal application approval number 20200629079), China.

CRediT authorship contribution statement

Jingyu Fang: Conceptualization, Investigation, Formal analysis, Writing – original draft. **Yang Lin:** Conceptualization, Writing – review & editing. **Hualing Xie:** Conceptualization, Investigation. **Mohamed A. Farag:** Conceptualization, Writing – review & editing. **Simin Feng:** Conceptualization, Writing – review & editing, Funding acquisition. **Jinjun Li:** Conceptualization, Resources. **Ping Shao:** Conceptualization, Methodology, Supervision, Conceptualization, Funding acquisition.

Declaration of Competing Interest

The authors declare that they have no known competing financial interests or personal relationships that could have appeared to influence the work reported in this paper.

Appendix A. Supplementary data

Supplementary data to this article can be found online at https://doi.org/10.1016/j.fochx.2022.100207.

References

Canani, R. B., Costanzo, M. D., Leone, L., Pedata, M., Meli, R., & Calignano, A. (2011). Potential beneficial effects of butyrate in intestinal and extraintestinal diseases. *World J Gastroenterol, 17*(12), 1519–1528. https://doi.org/10.3748/wjg.v17.i12.1519

Chen, J., Li, L., Zhou, X., Sun, P., Li, B., & Zhang, X. (2018). Preliminary characterization and antioxidant and hypoglycemic activities in vivo of polysaccharides from Huidouba. *Food Funct, 9*(12), 6337–6348. https://doi.org/10.1039/c8fo01117f

Chen, Y., Liu, D., Wang, D., Lai, S., Zhong, R., Liu, Y., … Zhao, C. (2019). Hypoglycemic activity and gut microbiota regulation of a novel polysaccharide from Grifola frondosa in type 2 diabetic mice. *Food Chem Toxicol, 126*, 295–302. https://doi.org/10.1016/j.fct.2019.02.034

de Oliveira, G. L. V. (2019). The Gut Microbiome in Autoimmune Diseases. In Microbiome and Metabolome in Diagnosis, Therapy, and other Strategic Applications, (pp. 325-332).

Elshahed, M. S., Miron, A., Aprotosoaie, A. C., & Farag, M. A. (2021). Pectin in diet: Interactions with the human microbiome, role in gut homeostasis, and nutrient-drug interactions. *Carbohydr Polym, 255*, Article 117388. https://doi.org/10.1016/j.carbpol.2020.117388

Fan, Y., & Pedersen, O. (2021). Gut microbiota in human metabolic health and disease. *Nat Rev Microbiol, 19*(1), 55–71. https://doi.org/10.1038/s41579-020-0433-9

Fecka, I., Nowicka, A., Kucharska, A. Z., & Sokół-Łętowska, A. (2021). The effect of strawberry ripeness on the content of polyphenols, cinnamates, L-ascorbic and carboxylic acids. *Journal of Food Composition and Analysis, 95*. https://doi.org/10.1016/j.jfca.2020.103669

Fu, X., Liu, Z., Zhu, C., Mou, H., & Kong, Q. (2019). Nondigestible carbohydrates, butyrate, and butyrate-producing bacteria. *Crit Rev Food Sci Nutr, 59*(sup1), S130–S152. https://doi.org/10.1080/10408398.2018.1542587

Gao, H., Wen, J. J., Hu, J. L., Nie, Q. X., Chen, H. H., Xiong, T., … Xie, M. Y. (2018). Polysaccharide from fermented Momordica charantia L. with Lactobacillus plantarum NCU116 ameliorates type 2 diabetes in rats. *Carbohydr Polym, 201*, 624–633. https://doi.org/10.1016/j.carbpol.2018.08.075

Gastaldelli, A., Gaggini, M., & DeFronzo, R. A. (2017). Role of adipose tissue insulin resistance in the natural history of type 2 diabetes: results from the San Antonio metabolism study. *Diabetes, 66*(4), 815–822. https://doi.org/10.2337/db16-1167

Hsieh, Y. S., Chien, C., Liao, S. K., Liao, S. F., Hung, W. T., Yang, W. B., … Wong, C. H. (2008). Structure and bioactivity of the polysaccharides in medicinal plant *Dendrobium huoshanense*. *Bioorg Med Chem, 16*(11), 6054–6068. https://doi.org/10.1016/j.bmc.2008.04.042

Jia, L., Li, D., Feng, N., Shamoon, M., Sun, Z., Ding, L., … Chen, Y. Q. (2017). Anti-diabetic Effects of Clostridium butyricum CGMCC0313.1 through Promoting the Growth of Gut Butyrate-producing Bacteria in Type 2 Diabetic Mice. *Sci Rep, 7*(1), 7046. https://doi.org/10.1038/s41598-017-07335-0

Kasahara, K., Krautkramer, K. A., Org, E., Romano, K. A., Kerby, R. L., Vivas, E. I., … Rey, F. E. (2018). Interactions between Roseburia intestinalis and diet modulate atherogenesis in a murine model. *Nat Microbiol, 3*(12), 1461–1471. https://doi.org/10.1038/s41564-018-0272-x

Ke, Y., Zhan, L., Lu, T., Zhou, C., Chen, X., Dong, Y., … Chen, S. (2020). Polysaccharides of *Dendrobium officinale Kimura & Migo* Leaves Protect Against Ethanol-Induced Gastric Mucosal Injury via the AMPK/mTOR Signaling Pathway in Vitro and vivo. *Front Pharmacol, 11*, Article 526349. https://doi.org/10.3389/fphar.2020.526349

Kjolbaek, L., Benitez-Paez, A., Gomez Del Pulgar, E. M., Brahe, L. K., Liebisch, G., Matysik, S., … Sanz, Y. (2020). Arabinoxylan oligosaccharides and polyunsaturated fatty acid effects on gut microbiota and metabolic markers in overweight individuals with signs of metabolic syndrome: A randomized cross-over trial. *Clin Nutr, 39*(1), 67–79. https://doi.org/10.1016/j.clnu.2019.01.012

Kobayashi, M., Mikami, D., Kimura, H., Kamiyama, K., Morikawa, Y., Yokoi, S., … Iwano, M. (2017). Short-chain fatty acids, GPR41 and GPR43 ligands, inhibit TNF-alpha-induced MCP-1 expression by modulating p38 and JNK signaling pathways in human renal cortical epithelial cells. *Biochem Biophys Res Commun, 486*(2), 499–505. https://doi.org/10.1016/j.bbrc.2017.03.071

Kuang, M. T., Li, J. Y., Yang, X. B., Yang, L., Xu, J. Y., Yan, S., … Zhou, J. (2020). Structural characterization and hypoglycemic effect via stimulating glucagon-like peptide-1 secretion of two polysaccharides from *Dendrobium officinale*. *Carbohydr Polym, 241*, Article 116326. https://org/10.1016/j.carbpol.2020.116326.

Lee, S. M., Kim, N., Nam, R. H., Park, J. H., Choi, S. I., Park, L., … D. h.. (2019). Gut microbiota and butyrate level changes associated with the long-term administration of proton pump inhibitors to old rats. *Sci Rep, 9*(1), 6626. https://org/10.1038/s41598-019-43112-x.

Liang, L., Liu, G., Zhang, F., Li, Q., & Linhardt, R. J. (2020). Digestibility of squash polysaccharide under simulated salivary, gastric and intestinal conditions and its impact on short-chain fatty acid production in type-2 diabetic rats. *Carbohydr Polym, 235*, Article 115904. https://doi.org/10.1016/j.carbpol.2020.115904

Liu, J., Li, H., Gong, T., Chen, W., Mao, S., Kong, Y., … Sun, J. (2020). Anti-neuroinflammatory Effect of Short-Chain Fatty Acid Acetate against Alzheimer's Disease via Upregulating GPR41 and Inhibiting ERK/JNK/NF-kappaB. *J Agric Food Chem, 68*(27), 7152–7161. https://doi.org/10.1021/acs.jafc.0c02807

Luck, H., Khan, S., Kim, J. H., Copeland, J. K., Revelo, X. S., Tsai, S., … Winer, D. A. (2019). Gut-associated IgA(+) immune cells regulate obesity-related insulin resistance. *Nat Commun, 10*(1), 3650. https://org/10.1038/s41467-019-11370-y.

Moini, J. (2019). Pathophysiology of Diabetes. In Epidemiology of Diabetes, (pp. 25-43).

Møller, A. K., Søborg, D. A., Abu Al-Soud, W., Sørensen, S. J., & Kroer, N. (2013). Bacterial community structure in High-Arctic snow and freshwater as revealed by pyrosequencing of 16S rRNA genes and cultivation. *Polar Research, 32*(1). https://org/10.3402/polar.v32i0.17390.

Puddu, A., Sanguineti, R., Montecucco, F., & Viviani, G. L. (2014). Evidence for the gut microbiota short-chain fatty acids as key pathophysiological molecules improving diabetes. *Mediators Inflamm, 14*, Article 162021. https://org/10.1155/2014/162021.

Pylkas, A., Juneja, L., & Slavin, J. (2005). Comparison of Different Fibers for In Vitro Production of Short Chain Fatty Acids by Intestinal Microflora. *Journal of medicinal food, 8*, 113–116. https://org/10.1089/jmf.2005.8.113.

Quast, C., Pruesse, E., Yilmaz, P., Gerken, J., Schweer, T., Yarza, P., … Glockner, F. O. (2013). The SILVA ribosomal RNA gene database project: Improved data processing and web-based tools. *Nucleic Acids Res, 41*, D590–D596. https://org/10.1093/nar/gks1219.

Rao, P., & Pattabiraman, T. N. (1989). Reevaluation of the phenol-sulfuric acid reaction for the estimation of hexoses and pentoses. *Analytical Biochemistry, 181*(1), 18–22. https://org/10.1016/0003-2697(89)90387-4.

Ru, Y., Liu, K., Kong, X., Li, X., Shi, X., & Chen, H. (2020). Synthesis of selenylated polysaccharides from Momordica charantia L. and its hypoglycemic activity in streptozotocin-induced diabetic mice. *Int J Biol Macromol, 152*, 295–304. https://org/10.1016/j.ijbiomac.2020.02.288.

Shang, Z. Z., Qin, D. Y., Li, Q. M., Zha, X. Q., Pan, L. H., Peng, D. Y., & Luo, J. P. (2021). *Dendrobium huoshanense* stem polysaccharide ameliorates rheumatoid arthritis in mice via inhibition of inflammatory signaling pathways. *Carbohydr Polym, 258*, Article 117657. https://org/10.1016/j.carbpol.2021.117657.

Shin, N. R., Whon, T. W., & Bae, J. W. (2015). Proteobacteria: microbial signature of dysbiosis in gut microbiota. *Trends Biotechnol, 33*(9), 496–503. https://doi.org/10.1016/j.tibtech.2015.06.011

Song, L., Qu, D., Zhang, Q., Jiang, J., Zhou, H., Jiang, R., … Yan, H. (2017). Phytosterol esters attenuate hepatic steatosis in rats with non-alcoholic fatty liver disease rats fed a high-fat diet. *Sci Rep, 7*, 41604. https://org/10.1038/srep41604.

Sun, L., Xie, C., Wang, G., Wu, Y., Wu, Q., Wang, X., … Jiang, C. (2018). Gut microbiota and intestinal FXR mediate the clinical benefits of metformin. *Nat Med, 24*(12), 1919–1929. https://org/10.1038/s41591-018-0222-4.

Tolhurst, G., Heffron, H., Lam, Y., Parker, H., Habib, A., Diakogiannaki, E., … Gribble, F. (2011). Short-Chain Fatty Acids Stimulate Glucagon-Like Peptide-1 Secretion via the G-Protein–Coupled Receptor FFAR2. *Diabetes, 61*, 364–371. https://doi.org/10.2337/db11-1019

Tomas, M., Beekwilder, J., Hall, R. D., Diez Simon, C., Sagdic, O., & Capanoglu, E. (2018). Effect of dietary fiber (inulin) addition on phenolics and in vitro bioaccessibility of tomato sauce. *Food Res Int, 106*, 129–135. https://org/10.1016/j.foodres.2017.12.050.

Ulven, T. (2012). Short-chain free fatty acid receptors FFA2/GPR43 and FFA3/GPR41 as new potential therapeutic targets. *Front Endocrinol (Lausanne), 3*, 111. https://org/10.3389/fendo.2012.00111.

Wang, H. Y., Li, Q. M., Yu, N. J., Chen, W. D., Zha, X. Q., Wu, D. L., … Luo, J. P. (2019). *Dendrobium huoshanense* polysaccharide regulates hepatic glucose homeostasis and pancreatic beta-cell function in type 2 diabetic mice. *Carbohydr Polym, 211*, 39–48. https://org/10.1016/j.carbpol.2019.01.101.

Wang, Y. H. (2021). Traditional uses, chemical constituents, pharmacological activities, and toxicological effects of *Dendrobium* leaves: A review. *J Ethnopharmacol, 270*, Article 113851. https://org/10.1016/j.jep.2021.113851.

Xie, J. H., Shen, M. Y., Nie, S. P., Zhao, Q., Li, C., & Xie, M. Y. (2014). Separation of water-soluble polysaccharides from Cyclocarya paliurus by ultrafiltration process. *Carbohydr Polym, 101*, 479–483. https://org/10.1016/j.carbpol.2013.09.075.

Xie, S. Z., Ge, J. C., Li, F., Yang, J., Pan, L. H., Zha, X. Q., … Luo, J. P. (2018). Digestive behavior of *Dendrobium huoshanense* polysaccharides in the gastrointestinal tracts of mice. *Int J Biol Macromol, 107*, 825–832. https://doi.org/10.1016/j.ijbiomac.2017.09.047

Xie, S. Z., Liu, B., Ye, H. Y., Li, Q. M., Pan, L. H., Zha, X. Q., … Luo, J. P. (2019). *Dendrobium huoshanense* polysaccharide regionally regulates intestinal mucosal barrier function and intestinal microbiota in mice. *Carbohydr Polym, 206*, 149–162. https://org/10.1016/j.carbpol.2018.11.002.

Xie, S. Z., Yang, G., Jiang, X. M., Qin, D. Y., Li, Q. M., Zha, X. Q., … Luo, J. P. (2020). Polygonatum cyrtonema Hua Polysaccharide Promotes GLP-1 Secretion from Enteroendocrine L-Cells through Sweet Taste Receptor-Mediated cAMP Signaling. *J Agric Food Chem, 68*(25), 6864–6872. https://org/10.1021/acs.jafc.0c02058.

Yang, J., Chen, H., Nie, Q., Huang, X., & Nie, S. (2020a). *Dendrobium officinale* polysaccharide ameliorates the liver metabolism disorders of type II diabetic rats. *Int J Biol Macromol, 164*, 1939–1948. https://org/10.1016/j.ijbiomac.2020.08.007.

Yang, K., Lu, T., Zhan, L., Zhou, C., Zhang, N., Lei, S., … Chen, S. (2020b). Physicochemical characterization of polysaccharide from the leaf of *Dendrobium officinale* and effect on LPS induced damage in GES-1 cell. *Int J Biol Macromol, 149*, 320–330. https://org/10.1016/j.ijbiomac.2020.01.026.

Zhang, M., Wu, J., Han, J., Shu, H., & Liu, K. (2018). Isolation of polysaccharides from *Dendrobium officinale* leaves and anti-inflammatory activity in LPS-stimulated THP-1 cells. *Chem Cent J, 12*(1), 109. https://org/10.1186/s13065-018-0480-8.

Zhang, X., Luo, Y., Wei, G., Li, Y., Huang, Y., Huang, J., … Du, S. (2019). Physicochemical and Antioxidant Properties of the Degradations of Polysaccharides from Dendrobium officinale and Their Suitable Molecular Weight Range on Inducing HeLa Cell Apoptosis. *Evid Based Complement Alternat Med, 2019*, 4127360. https://doi.org/10.1155/2019/4127360

Zhu, L., Zhu, W., Zhao, T., Chen, H., Zhao, C., Xu, L., … Jiang, J. (2021). Environmental Temperatures Affect the Gastrointestinal Microbes of the Chinese Giant Salamander. *Front Microbiol, 12*, Article 543767. https://org/10.3389/fmicb.2021.543767.